applied optics

Physical compensation of phase curvature in digital holographic microscopy by use of programmable liquid lens

Ana Doblas,[1,2,*] Diego Hincapie-Zuluaga,[2,3] Genaro Saavedra,[1] Manuel Martínez-Corral,[1] and Jorge Garcia-Sucerquia[2]

[1]3D Imaging and Display Laboratory, Department of Optics, University of Valencia, E-46100 Burjassot, Spain
[2]Universidad Nacional de Colombia Sede Medellin, School of Physics, A.A: 3840-Medellin-050034, Colombia
[3]Metropolitan Technological Institute (ITM), A.A:3840-Medellin-050034, Colombia
*Corresponding author: a.isabel.doblas@uv.es

Received 26 March 2015; revised 12 May 2015; accepted 13 May 2015; posted 13 May 2015 (Doc. ID 236996); published 1 June 2015

Quantitative phase measurements obtained with digital holographic microscopes are strongly dependent on the optical arrangement of the imaging system. The nontelecentric operation provides phase measurements affected by a parabolic phase factor and requires numerical postprocessing, which does not always remove all the perturbation. Accurate phase measurements are achieved by using the imaging system in telecentric mode. Unfortunately, this condition is not accomplished when a commercial microscope is used as the imaging system. In this paper, we present an approach for obtaining accurate phase measurements in nontelecentric imaging systems without the need for numerical postprocessing. The method uses an electrically tunable liquid lens to illuminate the sample so that the perturbing parabolic wavefront is cancelled out. Experimental holograms of a Fresnel lens and a section of the thorax of a *Drosophila melanogaster* fly are captured to verify the proposed method.

OCIS codes: (090.1995) Digital holography; (110.0180) Microscopy; (110.2990) Image formation theory; (100.5070) Phase retrieval; (090.1000) Aberration compensation.

http://dx.doi.org/10.1364/AO.54.005229

1. INTRODUCTION

Phase perturbations can appear at the pupil and also at the image plane (IP) of an imaging system. Whereas pupil perturbations are responsible for the aberrations, image-plane perturbations are usually of no concern, as only intensity images are of interest. However, when imaging phase objects, the presence of phase perturbations in the image plane is typically an issue of concern.

Quantitative phase imaging (QPI) is a methodology that quantifies the phase of transparent samples by retrieving the complex wavefield at the image plane. In such a case, the presence of phase perturbations at the IP can ruin the measurements [1,2]. Among the multiple QPI architectures [3–6], digital holography microscopy (DHM) [7–10] is one of the most reputed. When DHM is implemented with a nontelecentric imaging system, it inherently suffers from a parabolic phase perturbation at the image plane. To remove the parabolic phase, different approaches have been proposed. Some methods are based on numerical *a posteriori* procedures [2,11–14]. Other techniques compensate the phase distortion and provide QPI without the effects introduced by the use of nontelecentric recording systems. The first approach is the use of twin-imaging systems for the reference and objects waves [15] to suppress *a priori* the residual quadratic phase factor. However, this method requires accurate alignment of the setup and also doubles the cost of the DHM. The other approach is achieved by performing a double-exposure technique. In this case, the phase distortion is removed *a posteriori* by subtracting the measured phase of a blank object from the measurement with the sample under research [16]. Although this method removes any phase distortion of the imaging system, the need for recording two holograms could not be convenient in microscopy applications in which dynamic processes are screened.

The natural way of performing single-shot QPI-DHM free of parabolic phase perturbation is based on the use of a telecentric imaging system [17–19]. Unfortunately, this solution cannot be implemented if one tries to use, as the imaging system of the DHM, a commercially available microscope. This is because, aiming to save space, commercial microscopes are usually mounted in a nontelecentric configuration. In such

cases, it is still possible to cancel out the parabolic phase, provided that the sample is illuminated with a specific spherical wavefront [15,20,21]. The problem of this solution is that the illumination architecture is fully adapted to the magnification of the microscope objective (MO). Then, it requires very accurate mechanical movement of the illumination system when the MO is changed.

The aim of this work is to report an alternative approach to avoid the phase perturbation introduced by nontelecentric DHMs. The proposal uses an electrically tunable liquid lens (LL) to illuminate the sample with the suitable spherical wavefront. The main advantage of using an LL is that the compensation can be achieved for any MO by tuning electronically the LL focal length. Although we validate the method in a QPI-DHM architecture, it could be utilized in any QPI methodology that gathers information through an imaging system.

2. BASIC THEORY

The optical configuration of a transmission off-axis DHM is illustrated in Fig. 1. Following a Mach–Zehnder architecture, the light proceeding from a laser of wavelength λ is collimated and split to produce the object (O) and reference (R) waves. In the object arm, an imaging system is inserted to image the sample. The imaging system is composed by an infinity-corrected MO and a tube lens (TL). The object is placed at the MO front focal plane. Whatever the distance between the MO and the TL, the image appears at the back focal plane of the TL. The later plane is named here as the IP.

At the IP, the interference between the wavefield scattered by the object, $U_{\mathrm{IP}}(\boldsymbol{x})$, and the tilted reference plane wave, $R(\boldsymbol{x})$, occurs. The complex distribution $U_{\mathrm{IP}}(\boldsymbol{x})$ can be derived by using ABCD transformations [22,23]. After straightforward algebra, we find that

$$U_{\mathrm{IP}}(\boldsymbol{x}) = \exp\left(i\frac{k}{2C}|\boldsymbol{x}|^2\right)\left\{O\left(\frac{\boldsymbol{x}}{M}\right) \otimes_2 \tilde{p}\left(\frac{\boldsymbol{x}}{\lambda f_{\mathrm{TL}}}\right)\right\}, \quad (1)$$

where $\boldsymbol{x} = (x, y)$ are the spatial transverse coordinates, $O(\mathbf{x})$ is the object transmittance, $\tilde{p}(\cdot)$ is the Fourier transform of the pupil transmittance, and $k = 2\pi/\lambda$ and $M = -f_{\mathrm{TL}}/f_{\mathrm{MO}}$ the magnification factor.

Apart from the 2D convolution, $\otimes_2$, typically associated to any imaging process, Eq. (1) also shows a quadratic phase factor whose radius of curvature is

$$C = \frac{f_{\mathrm{TL}}^2}{f_{\mathrm{TL}} - d} = \frac{f_{\mathrm{TL}}^2}{\Delta}. \quad (2)$$

This parabolic factor is inherent in imaging systems operating in a nontelecentric regime ($d \neq f_{\mathrm{TL}}$). As a result, the DHM intrinsically becomes a shift-variant system [18,19] and numerical postprocessing [2,11–14] is required to cancel out the effects of that perturbing phase.

The irradiance distribution recorded on the CCD, usually named as the hologram, is

$$H(\boldsymbol{x}) = |U_{\mathrm{IP}}(\boldsymbol{x})|^2 + |R(\boldsymbol{x})|^2 + U_{\mathrm{IP}}(\boldsymbol{x})R^*(\boldsymbol{x}) + U_{\mathrm{IP}}^*(\boldsymbol{x})R(\boldsymbol{x}). \quad (3)$$

As well known, in off-axis DHM, the object wavefront $U_{\mathrm{IP}}(\boldsymbol{x})$ is recovered by spatial filtering the third term from the Fourier transform of $H(\boldsymbol{x})$ [24]. Such a term spreads proportionally to $1/C$ and, therefore, is tightest when the DHM operates in telecentric mode [25].

Telecentricity is, then, the ideal imaging mode for DHM-QPI. However, the design of, for example, holographic modules [26] for their insertion in commercial, widefield microscopes, can face some mechanical constrains that could prevent the telecentricity of the system. In such cases, the best alternative is the insertion, in front of the specimen, of a converging lens that compensates the phase factor at the IP. In order to allow this compensation to be dynamic and to avoid mechanical movements, we propose here an electro-physical approach that uses an electrically tunable LL.

3. PHYSICAL COMPENSATION OF THE PARABOLIC PHASE PERTURBATION

Our approach consists of illuminating the sample with a converging spherical wave (see Fig. 2), whose curvature permits us to cancel out the quadratic phase at the IP [see Eq. (1)]. As seen in Fig. 2, the amplitude distribution at the specimen plane is given by

$$U_0(\boldsymbol{x}) = O(\boldsymbol{x})\exp(i k\boldsymbol{x}^2/2\mu), \quad (4)$$

where the radius of curvature

$$\mu = l - f_{\mathrm{LL}}, \quad (5)$$

l being the distance between the LL and the specimen.

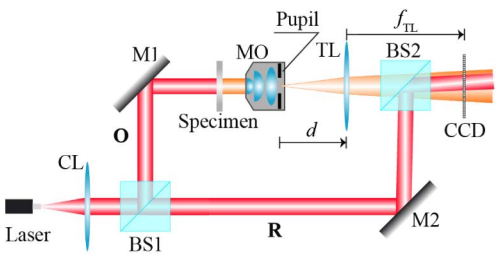

Fig. 1. Illustration of a transmission off-axis DHM when the configuration of the imaging system operates in nontelecentric mode. CL, collimating lens; BS1 and BS2, beam-splitter cubes; M1 and M2, mirrors; O, object wave; MO, microscope objective; TL, tube lens; CCD, charge-couple device; R, reference wave.

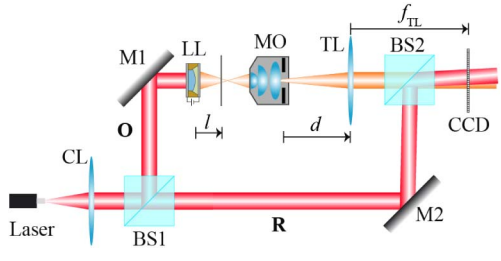

Fig. 2. Illustration of physical method for cancelling the phase perturbations in nontelencetric DHMs. The specimen is illuminated by a converging spherical wavefront. CL, collimating lens; BS1 and BS2, beam-splitter cubes; M1 and M2, mirrors; O, object wave; LL, electrically controlled liquid lens; MO, microscope objective; TL, tube lens; CCD, charge-couple device; R, reference wave.

For this setup, Eq. (1) can be rewritten as

$$U_{\mathrm{IP}}(\boldsymbol{x}) = \exp\left(\mathrm{i}\frac{k}{2C}|\boldsymbol{x}|^2\right) \times \left\{\left[O\left(\frac{\boldsymbol{x}}{M}\right)\exp\left(-\mathrm{i}\frac{k}{2\mu}\frac{|\boldsymbol{x}|^2}{M^2}\right)\right] \otimes_2 \tilde{p}\left(\frac{\boldsymbol{x}}{\lambda f_{\mathrm{TL}}}\right)\right\}. \quad (6)$$

Equation (6) describes an imaging system that, from a strict point of view, is not linear and shift-invariant (LSI). However, there are cases in which the system is LSI in very good approximation. This happens when the phase factor inside the square brackets is almost plane in comparison with the size of $O(x/M)$. Assuming this condition, the parabolic phase can be taken out from the 2D convolution to obtain

$$U_{\mathrm{IP}}(\boldsymbol{x}) = \exp\left(\mathrm{i}\frac{k}{2C}|\boldsymbol{x}|^2\right)\exp\left(-\mathrm{i}\frac{k}{2\mu}\frac{|\boldsymbol{x}|^2}{M^2}\right) \times \left\{O\left(\frac{\boldsymbol{x}}{M}\right) \otimes_2 \tilde{p}\left(\frac{\boldsymbol{x}}{\lambda f_{\mathrm{TL}}}\right)\right\}. \quad (7)$$

The pair of parabolic phase terms cancel each other out when $C = \mu M^2$. Taking into account Eq. (2), this happens when

$$\mu = \frac{f_{\mathrm{MO}}^2}{\Delta}. \quad (8)$$

In other words, the condition for the cancellation of parabolic phases at the IP is to illuminate the sample with a spherical wave such that its focus is conjugated with the front focus of the TL.

To ensure that the LL does not introduce significant aberration, we have previously measured the 3D irradiance PSF of a widefield microscope in which the LL has been inserted at its aperture stop and compared it with the native microscope (without LL). From the results reported in [27], it is clear that no significant aberration is added by inserting the LL.

To demonstrate the utility of our approach, we have recorded the hologram of the diffractive Fresnel lens. In the experiment, the imaging system was composed by a 4 × /0.2 MO, a TL of $f_{\mathrm{TL}} = 200$ mm, and a CCD sensor with 1024 × 1024 square pixels of 6.9 μm size. The nontelecentric configuration was adjusted so that $\Delta = 95$ mm. For the physical compensation, we inserted an ARCTIC 39N0 liquid lens (VARIOPTIC), which is based on electro-wetting technology [28–33]. The optical power of the ARTIC 39N0, which ranges from −5.0 m^{-1} to +15 m^{-1}, was adjusted to fulfill the condition of Eq. (8). In Fig. 3, we show the hologram and the raw phase (i.e., the phase distribution obtained after filtering out the +1 term and compensating the angle of the reference wave) for three different configurations: (a) the DHM working in telecentric mode; (b) the DHM working in nontelecentric mode; and (c) the DHM working in nontelecentric mode but with the parabolic phase compensated physically with the LL.

If we compare the raw phase image for the telecentric DHM with the one for the nontelecentric DHM with physical compensation, we verify that the results obtained with our approach are totally comparable with those provided by the telecentric DHM and superior to those obtained with the nontelecentric one.

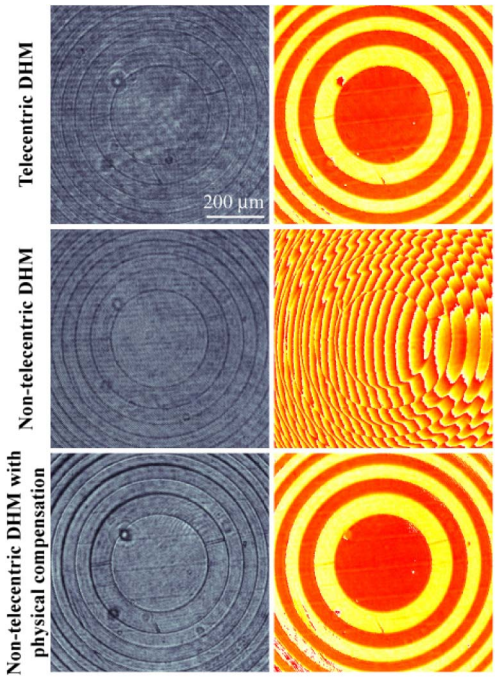

Fig. 3. Recorded hologram (left column) and row-phase image (right column) of a Fresnel lens, obtained with telecentric DHM (first row); nontelecentric DHM (second row); and nontelecentric DHM with physical compensation (bottom row).

For better comparison between the recovered raw phases produced by the telecentric-DHM and the electrophysical DHM, we have plotted in Fig. 4 the phase profiles of the Fresnel lens along its center. We find that the two methods provide results with comparable accurateness.

Finally, we have tested our method with a biological sample: the thorax of a *Drosophila melanogaster* fly. To record the hologram, we used a 10 × /0.45 MO and a TL of $f_{\mathrm{TL}} = 200$ mm.

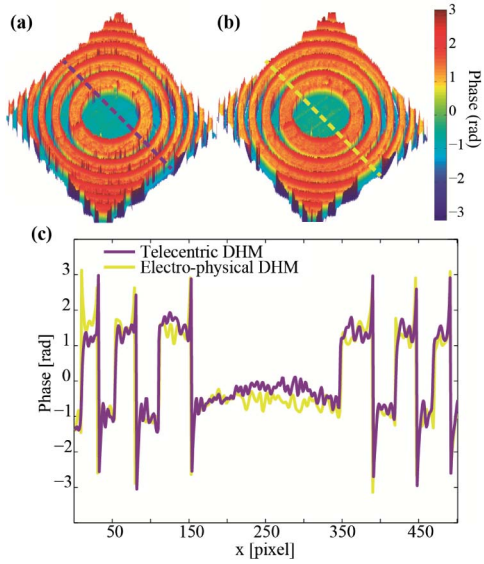

Fig. 4. Pseudocolored phase maps obtained with (a) the telecentric DHM and (b) the electrophysical DHM. Phase value along a line passing through the center is also plotted in panel (c).

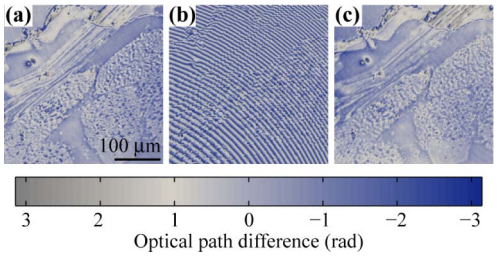

Fig. 5. Raw phases of a section of the thorax of a *Drosophila melanogaster* fly for (a) telecentric-DHM, (b) nontelecentric DHM, and (c) electrophysical DHM.

The raw phases are depicted in Fig. 5 for (a) the telecentric DHM, (b) the nontelecentric DHM with $\Delta = 50$ mm, and (c) the electrophysical DHM with the same offset Δ. Again, the raw phase images are recovered by spatial filtering the Fourier transform of the hologram and compensating the reference wave. Also in this experiment, we can confirm that the proposed approach provides phase measurement with the same accuracy as telecentric DHM and also without need of numerical postprocessing.

4. CONCLUSIONS

We have shown that the phase perturbations introduced by a nontelecentric imaging system can be fully eliminated by an electro-physically procedure. Inserting an electrically tunable LL in the illumination path, the perturbing phase is cancelled out at the image plane. By tuning the voltage of the LL, it is easy to produce the spherical illumination adapted to any of the interchangeable MOs of the microscope. We have demonstrated, experimentally, the utility of our proposal with a test object and also with a biological specimen. In both cases, we have shown that the electro-physical DHM produces QPI with the same accuracy as the telecentric DHM and is clearly superior to nontelecentric DHM.

Autonomous Government of Valencia (PROMETEOII/2014/072); Spanish Ministry of the Economy and Competitiveness (DPI2012-32994).

A. Doblas acknowledges funding from University of Valencia (predoctoral program "Atracció de Talent") and from Universidad Nacional de Colombia Sede Medellín. J. Garcia-Sucerquia and Diego Hincapie acknowledge the support from Universidad Nacional de Colombia (Hermes grant 19384), the Programa de Internacionalización del Conocimiento and Instituto Tecnológico Metropolitano—ITM (project number P14217).

REFERENCES

1. E. Cuche, P. Marquet, and C. Depeursinge, "Simultaneous amplitude-contrast and quantitative phase-contrast microscopy by numerical reconstruction of Fresnel off-axis holograms," Appl. Opt. **38**, 6994–7001 (1999).
2. T. Colomb, F. Montfort, J. Kühn, N. Aspert, E. Cuche, A. Marian, F. Charriere, S. Bourquin, P. Marquet, and C. Depeursinge, "Numerical parametric lens for shifting, magnification, and complete aberration compensation in digital holographic microscopy," J. Opt. Soc. Am. A **23**, 3177–3190 (2006).
3. A. Barty, K. A. Nugent, D. Paganin, and A. Roberts, "Quantitative optical phase microscopy," Opt. Lett. **23**, 817–819 (1998).
4. C. J. R. Sheppard, "Three-dimensional phase imaging with the intensity transport equation," Appl. Opt. **41**, 5951–5955 (2002).
5. B. Bhaduri, H. Pham, M. Mir, and G. Popescu, "Diffraction phase microscopy with white light," Opt. Lett. **37**, 1094–1096 (2012).
6. B. Bhaduri, K. Tangella, and G. Popescu, "Fourier phase microscopy with white light," Biomed. Opt. Express **4**, 1434–1441 (2013).
7. T. Kreis, *Handbook of Holographic Interferometry* (Wiley, 2004).
8. M. K. Kim, "Principles and techniques of digital holographic microscopy," SPIE Rev. **1**, 018005 (2010).
9. G. Popescu, *Quantitative Phase Imaging of Cells and Tissues* (McGraw-Hill, 2011).
10. P. Picart and J.-C. Li, *Digital Holography* (Wiley, 2012).
11. T. Colomb, J. Kühn, F. Charriere, and C. Depeursinge, "Total aberrations compensation in digital holographic microscopy with a reference conjugated hologram," Opt. Express **14**, 4300–4306 (2006).
12. J. Di, J. Zhao, W. Sun, H. Jiang, and X. Yan, "Phase aberration compensation of digital holographic microscopy based on least squares surface fitting," Opt. Commun. **282**, 3873–3877 (2009).
13. K. W. Seo, Y. S. Choi, E. S. Seo, and S. J. Lee, "Aberration compensation for objective phase curvature in phase holographic microscopy," Opt. Lett. **37**, 4976–4978 (2012).
14. Z. Wang, W. Qu, Y. Wen, F. Yang, and A. Asundi, "A new phase error compensation method in digital holographic microscopy," Proc. SPIE **9302**, 93023M (2015).
15. C. J. Mann, L. Yu, C.-M. Lo, and M. K. Kim, "High-resolution quantitative phase-contrast microscopy by digital holography," Opt. Express **13**, 8693–8698 (2005).
16. P. Ferraro, S. De Nicola, A. Finizio, G. Coppola, S. Grilli, C. Magro, and G. Pierattini, "Compensation of the inherent wave front curvature in digital holographic coherent microscopy for quantitative phase-contrast imaging," Appl. Opt. **42**, 1938–1946 (2003).
17. E. Sánchez-Ortiga, P. Ferraro, M. Martínez-Corral, G. Saavedra, and A. Doblas, "Digital holographic microscopy with pure-optical spherical phase compensation," J. Opt. Soc. Am. A **28**, 1410–1417 (2011).
18. A. Doblas, E. Sánchez-Ortiga, M. Martínez-Corral, G. Saavedra, P. Andrés, and J. Garcia-Sucerquia, "Shift-variant digital holographic microscopy: inaccuracies in quantitative phase imaging," Opt. Lett. **38**, 1352–1354 (2013).
19. A. Doblas, E. Sánchez-Ortiga, M. Martínez-Corral, G. Saavedra, and J. Garcia-Sucerquia, "Accurate single-shot quantitative phase imaging of biological specimens with telecentric digital holographic microscopy," J. Biomed. Opt. **19**, 46022 (2014).
20. W. Qu, C. O. Choo, V. R. Singh, Y. Yingjie, and A. Asundi, "Quasi-physical phase compensation in digital holographic microscopy," J. Opt. Soc. Am. A **26**, 2005–2011 (2009).
21. Y.-K. Chew, M.-T. Shiu, J.-C. Wang, and C.-C. Chang, "Compensation of phase aberration by using a virtual confocal scheme in digital holographic microscopy," Appl. Opt. **53**, G184–G191 (2014).
22. S. A. Collins, "Lens-system diffraction integral written in terms of matrix optics," J. Opt. Soc. Am. **60**, 1168–1177 (1970).
23. D. S. Goodman, "General principles of geometrical optics," in *Handbook of Optics*, M. Bass, ed., 2nd ed. (McGraw-Hill, 1995).
24. E. Cuche, P. Marquet, and C. Depeursinge, "Spatial filtering for zero-order and twin-image elimination in digital off-axis holography," Appl. Opt. **39**, 4070–4075 (2000).
25. E. Sánchez-Ortiga, A. Doblas, G. Saavedra, M. Martínez-Corral, and J. Garcia-Sucerquia, "Off-axis digital holographic microscopy: practical design parameters for operating at diffraction limit," Appl. Opt. **53**, 2058–2066 (2014).
26. E. Sánchez-Ortiga, A. Doblas, G. Saavedra, M. Martínez-Corral, and J. Garcia-Sucerquia, "Microscope, method and computer program for obtaining quantitative study of transparent samples by digital holographic microscopy," Spanish patent ES 2 534 960 A1 (April30, 2015).
27. M. Martínez-Corral, P. Y. Hsieh, A. Doblas, E. Sánchez-Ortiga, G. Saavedra, and Y. P. Huang, "Fast axial three-dimensional wide-field

microscopy with constant magnification and resolution," J. Disp. Technol., doi: 10.1109/JDT.2015.2404347 (to be published).
28. B. Berge and J. Peseux, "Variable focal lens controlled by an external voltage: an application of electrowetting," Eur. Phys. J. E **3**, 159–163 (2000).
29. C. Quilliet and B. Berge, "Electrowetting: a recent outbreak," Curr. Opin. Colloid Interface Sci. **6**, 34–39 (2001).
30. S. Grilli, L. Miccio, V. Vespini, A. Finizio, S. De Nicola, and P. Ferraro, "Liquid micro-lens array activated by selective electrowetting on lithium niobate substrates," Opt. Express **16**, 8084–8093 (2008).
31. L. Miccio, A. Finizio, S. Grilli, V. Vespini, M. Paturzo, S. De Nicola, and P. Ferraro, "Tunable liquid microlens arrays in electrode-less configuration and their accurate characterization by interference microscopy," Opt. Express **17**, 2487–2499 (2009).
32. D. Wang, Q. H. Wang, C. Shen, X. Zhou, and C. M. Liu, "Active optical zoom system," Appl. Opt. **53**, 7402–7406 (2014).
33. C.-J. Kim, M. Chang, M. Lee, J. Kim, and Y. H. Won, "Depth plane adaptive integral imaging using a varifocal liquid lens array," Appl. Opt. **54**, 2565–2571 (2015).